

# 超声振动对电火花表面强化的作用

张平<sup>1</sup>, 马琳<sup>1,2</sup>, 梁志杰<sup>1</sup>

(1. 装甲兵工程学院 再制造科技重点实验室, 北京 100072; 2. 防化指挥工程学院, 北京 102205)

**摘要:** 超声辅助电火花表面强化技术是电火花表面强化技术基础上发展起来的, 将超声引入电火花表面强化可以得到质量更高的表面强化层. 通过在45钢基体上添加超声振动, 实现电火花表面强化过程, 并据此研究超声对电火花表面强化技术的促进作用. 结果表明, 超声振动能够扩大电火花表面强化技术的强化层成形工艺区间, 获得表面形貌更加均匀的强化层. 同时超声振动将电火花表面强化技术的最大沉积效率提高了30%, 晶粒尺寸减小了24.18%, 显微硬度提高了10%. 超声振动扩大了热影响区的范围, 并将热影响区的硬度提高至基体以上. 超声辅助电火花表面强化获得的结合面有更好的耐腐蚀性能.

**关键词:** 超声振动; 电火花; 表面强化; 成形性; 强化层

**中图分类号:** TG455 **文献标识码:** A **文章编号:** 0253-360X(2011)03-0037-04



张平

## 0 序 言

电火花表面强化技术为工件的修复提供了节能环保的有效途径, 但是现有的电火花表面强化技术仍然存在着沉积效率低等工艺缺点, 而工艺参数的优化对沉积质量的提高十分有限, 因此复合电火花表面强化工艺相继出现<sup>[1-5]</sup>. 超声辅助电火花表面强化技术由于超声与电火花强化加工的同步性在工艺上更具优势, 已经有研究表明在沉积过程中添加超声振动, 实现超声辅助电火花表面强化使表面强化质量有明显提高, 但是现有研究均未对其进行深入探讨尤其是其强化机理<sup>[6]</sup>. 文中在传统便携式电火花表面强化(ESD)设备基础上添加超声振动装置, 使得基体能够进行超声振动, 实现超声辅助电火花表面强化(UAESD), 并由此展开试验, 研究超声振动对电火花表面强化技术的作用. 希望超声振动的添加能够为电火花表面强化技术的发展带来新的契机.

## 1 超声辅助电火花强化的实现

试验选取的电火花表面强化设备为课题组自行研制的便携式电火花冷补机, 该设备可实现对保护气流、输出功率、输出电压、电极转速四个工艺参数

的调整. 试验证明利用该设备采用合适的电火花沉积工艺可以得到性能优秀的表面强化层. 在此设备的基础上通过在工件上添加超声振动实现超声辅助电火花表面强化过程, 图1为试验采用的超声辅助电火花表面强化的过程原理图.

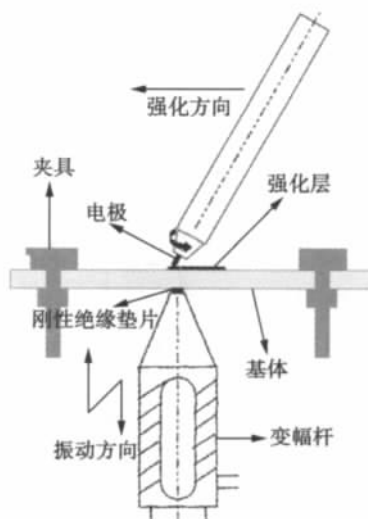


图1 超声辅助电火花表面强化过程示意图

Fig. 1 Diagram of ultra-assisted electrode spark depositing process

从图1中可以看出, 在电火花表面强化过程中, 电极在沿强化方向进行运动的同时自身也在进行旋转, 而工件基体的超声振动是通过变幅杆传递给基

体的,基体的振动方向是纵向上下振动,正好与工件加工表面垂直.试验以镍基合金 AT-ERNI818 为电极,45 钢板材为基体,强化时间为 30 min,强化面积为  $1\text{ cm} \times 1\text{ cm}$ .

## 2 超声振动对电火花成形性的影响

试验发现,当保护气流一定时,输出功率和电压对强化层的影响最为重要,而其电极转速的影响就相对很弱.在该设备的可调范围内,其它工艺不变的情况下只改变电极转速不会对强化层的成形性产生影响.故此,在对成形性的探讨过程中只研究输出功率和输出电压两个主要参数,表 1、表 2 分别为普通电火花表面强化和超声辅助电火花表面强化的成形结果.

表 1 普通电火花表面强化成形结果  
Table 1 Formability of ESD

电压 $U/V$	功率 $P/kW$					
	0.3	0.6	0.9	1.2	1.5	1.8
95	○	○	○	○	○	○
130	○	○	○	○	●	●
145	○	○	●	●	●	●
180	○	●	●	●	●	●

表 2 超声辅助电火花表面强化的成形结果  
Table 2 Formability of UAESD

电压 $U/V$	功率 $P/kW$					
	0.3	0.6	0.9	1.2	1.5	1.8
95	○	○	○	○	○	○
130	○	○	○	○	○	●
145	○	○	○	○	○	●
180	○	○	○	○	○	●

(表中○表示可以成形;●缺陷孔洞明显不能成形)

从表 1,表 2 中可以看出超声的添加极大的扩大了电火花表面强化的工艺成形范围.表 1 中的结果显示,当输出功率和输出电压达到一定值时会导致电极过热,所以强化层无法成形.而超声的振动使得一部分热能转变为振动机械能,损耗掉了电极材料上过多的能量,促进了电火花表面强化的成形过程,扩大了电火花表面强化的工艺成形范围.

图 2 显示的是普通电火花表面强化和超声辅助电火花表面强化所获得强化层的表面形貌.图 2a,b 是在相同的工艺条件下获得的强化层,当电火花表面强化技术无法成形时,超声振动的添加可以使强化层成形,而当电火花表面强化技术可以成形时,超

声的添加可以获得更好的表面形貌.图 2c 表面强化层的平均厚度相同,而利用超声辅助电火花表面强化技术获得的强化层表面的均匀性要明显好于传统的电火花表面强化技术.由于超声振动促进了熔池内各元素的运动,提高了熔融态电极材料表面的流动性,从而提高了强化层的表面质量.

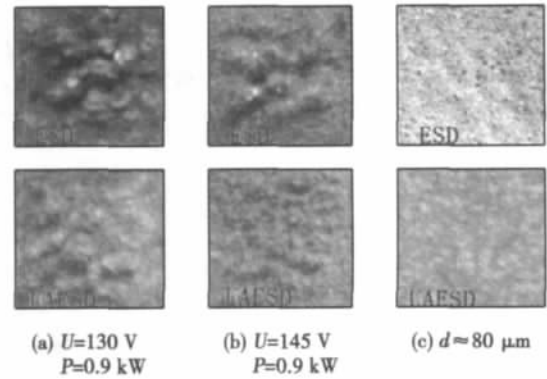


图 2 电火花表面强化层形貌

Fig. 2 Surface images of coating

试验过程中发现,相同工艺参数下,超声辅助电火花所获得的强化层厚度要低于普通电火花表面强化层的厚度.但是,在可成形的范围内研究发现,当  $P=0.6\text{ kW}$ ,  $U=145\text{ V}$  时,普通电火花表面强化所获得的强化层厚度最大,平均厚度为  $1\ 280\ \mu\text{m}$ ;当  $P=1.5\text{ kW}$ ,  $U=180\text{ V}$  时,超声辅助电火花表面强化所获得的强化层厚度最大,平均厚度为  $1\ 960\ \mu\text{m}$ .由此,若以提高沉积效率为目的,超声的添加可使得沉积效率提高约 30%.

在相同的工艺参数条件下,超声振动会对基体和电极材料产生影响,超声振动会加速热量的传导,减少强化过程中电极材料用以熔化形成覆层的热量,另外,机械振动的同时也会加速强化过程中材料的飞溅.因此,相同工艺参数条件下超声辅助电火花表面强化的沉积效率要低于普通的电火花表面强化技术.而继续加大输出功率或者输出电压,对于普通电火花表面强化技术而言已无法形成强化层.然而,此时超声辅助电火花表面强化却仍然可以在基体表面形成强化层,沉积效率也随着输出功率或输出电压的增加而增加.

## 3 超声振动对电火花强化层性能影响

选取强化层厚度接近的两个覆层截面作为研究对象,利用显微硬度计对覆层和基体热影响区的显微硬度进行测量,得到的结果如图 3 所示.

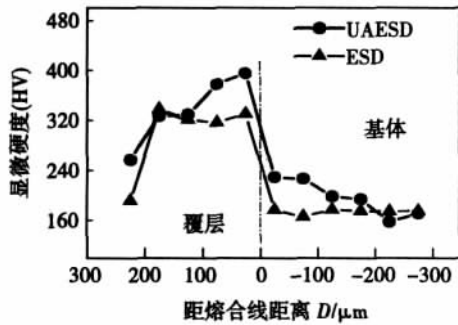


图 3 电火花表面强化截面显微硬度分布

Fig. 3 Microhardness distribution of cross-section of coating

从图 3 中可以看出超声的添加使强化层和热影响区的硬度都有所提高. 由于超声作用在基体上, 因此越靠近熔合线超声的作用越明显, 另外超声的添加降低了热影响区的硬度梯度, 提高了熔合线附近的材料硬度.

对覆层截面进行腐蚀, 观察其金相组织, 得到图 4. 在硝酸、酒精的腐蚀下, 45 钢基体的晶粒非常明显, 而强化层并无明显变化. 将强化层进行电解腐蚀, 发现强化层在金相显微镜下放大 500 倍, 可以看到呈扁平状的结构. 在添加了超声辅助作用下的电火花表面强化层中, 扁平状结构拉得更加扁平, 从侧面说明了强化层晶粒在一定程度上得到了细化. 图 4a 中, 强化层和基体熔合线处腐蚀严重, 表现为

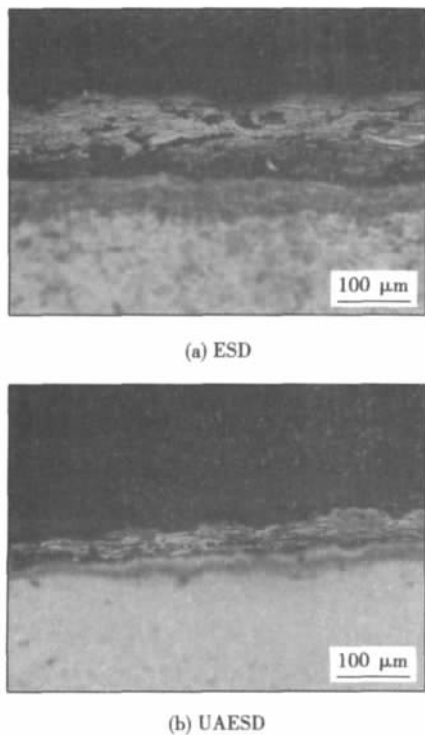


图 4 电火花表面强化截面金相组织  
Fig. 4 Microstructures of cross-section

较宽黑色“凹坑带”, 而图 4b 中, 熔合线虽然也出现了腐蚀痕迹, 但是其“凹坑带”明显变窄, 证明了在超声的作用下强化层和基体的相互熔合更加致密, 图 3 中, 超声辅助电火花表面强化熔合线附近的显微硬度略高于普通电火花表面强化熔合线附近的显微硬度, 也证明了超声的添加促进了强化层和基体相互熔合.

采用 XRD 对强化层表面成分进行分析, 得到图 5. 从图 5 中可以看出, 添加了超声的电火花表面强化的峰宽要小于未添加超声的电火花表面强化层的峰宽, 这说明晶粒在一定程度上得到了细化.

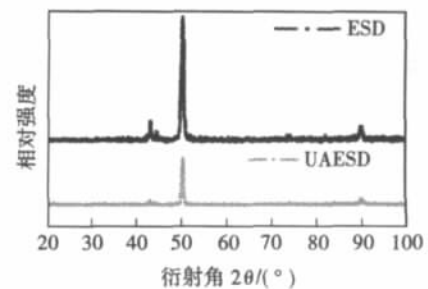


图 5 电火花表面强化层 XRD 分析  
Fig. 5 XRD patterns of coating

根据谢勒公式对三个峰值点的晶粒进行计算, 普通电火花表面沉积时, 得到的强化层表面晶粒大小约为 29.57 nm, 而添加了超声振动的表面晶粒大小约为 22.42 nm, 比未添加超声振动时的大小减少了约 24.18%. 而对强化层表面的硬度测量显示未添加超声振动的强化层表面显微硬度约为 326.87 HV, 而添加了超声振动的强化层表面的显微硬度提高到了 358.27 HV. 该硬度比未添加超声振动时提高了 10%, 是 45 钢基体的 2.2 倍.

#### 4 超声振动对电火花强化作用机理的探讨

对涂层的测量表明, 超声的添加对电火花表面强化具有一定的促进作用. 在获得相同厚度强化层的情况下, 超声辅助电火花表面强化得到的强化层表面成形性更好, 晶粒尺寸有所降低, 强化层硬度也获得了提高. 虽然超声的促进作用已经证实, 但是对其机理的研究尚基本空白, 现根据试验结果结合超声在其它加工技术中的作用原理, 及其对电火花表面强化的作用机理进行尝试性探讨, 认为超声的强化作用可能通过以下两个方面实现.

(1) 超声的机械作用. 超声振动直接作用在基体上,能够对基体产生冲击,由于基体为钢性板材,故此该冲击作用可以直达基材表面,当电极材料熔化在基体表面形成强化层时,超声对熔池部分也会产生作用,该振动可能直接对电极材料的凝固成形及其与基体的结合产生影响. 对于结合面首先超声振动能够破坏材料表面的氧化层,增加熔滴与基体的润湿性,从而促进其冶金结合<sup>[6,7]</sup>. 同时超声振动能够降低反应势垒<sup>[8]</sup>,促进电极材料和基体材料组元的扩散运动,也能起到增强基材与电极冶金结合的作用. 对于强化层,在电极材料熔化形核的过程中,超声具有“高速搅拌”<sup>[8]</sup>效应,使晶粒得到细化.

(2) 超声的热作用. 超声对电火花表面强化热作用在强化过程中的成形上体现的最为明显. 在电火花强化过程中,为了提高加工效率,经常加大输出功率,从而导致了电极材料的过热而大量熔化,在基材表面形成蜂窝状覆层,无法成形. 而超声是一种能量波,它的引入显著加快热传导过程,增强熔透性<sup>[9]</sup>,将多余的能量向接触点周围传播,从而减少了电极材料的过热情况,促进了强化层的成形. 同样也是由于超声振动的传热作用,使得接触点周围的热量分布更加均匀,晶粒的长大更加均匀.

## 5 结 论

(1) 超声振动扩大了电火花表面强化技术的强化层成形工艺区间,可以获得表面形貌更加均匀的强化层.

(2) 超声振动将电火花表面强化技术的最大沉积效率提高了 30%,显微硬度提高了 10%. 计算表明超声将强化层的晶粒尺寸减少了约 24.18%,同时超声振动扩大了热影响区的范围,热影响区内的硬度也有所提高.

(3) 电解腐蚀的结果表明,超声辅助电火花表面强化获得的结合面有更好的耐腐蚀性能.

## 参考文献:

- [1] Di P, Gu W S, Zhu S G. Effect of electrospark alloying process on microstructure and properties of the coating [J]. *Journal of Dong Hua University*, 2002, 19, 95 - 97.
- [2] 任 亮, 刘道新, 张晓化, 等. Mo 电极电火花强化与喷丸复合提高 Ti 合金微动疲劳抗力 [J]. *中国有色金属学报*, 2007, 17, 2017 - 2022.  
Ren Liang, Liu Daoxin, Zhang Xiaohua, *et al.* Electrospark surface strengthening by Mo electrode and shot peening on improving fretting fatigue resistance of Ti alloy [J]. *The Chinese Journal of Nonferrous Metals*, 2007, 17, 2017 - 2022.
- [3] 方 宇. 液中放电沉积关键技术研究 [D]. 哈尔滨: 哈尔滨工业大学, 2006.
- [4] Katsushi F, Akinori, Hideki T, *et al.* Accretion of titanium carbide by electrical discharge machining with powder suspended in working fluid [J]. *Precision Engineering Journal of the International Societies for Precision Engineering and Nanotechnology*, 2001, 25, 38 - 144.
- [5] 朱 健, 张全忠, 张立文, 等. 钛合金表面电火花沉积 WC 涂层的研究 [J]. *金属热处理*, 2005, 30, 11 - 14.  
Zhu Jian, Zhang Quanzhong, Zhang Liwen, *et al.* WC coating deposited on the surface of titanium alloy by electrospark process [J]. *Heat Treatment of Metals*, 2005, 30, 11 - 14.
- [6] Kin Ming Kwan. Investigation of effects of ultrasonic vibration of wetting, heating and curing of structure adhesives [D]. Dissertation for Doctor Degree. USA: the Ohio State University, 2000.
- [7] Xu Z W, Yan J C, Zhang B Y, *et al.* Behaviors of oxide film at the ultrasonic aided interaction interface of Zn-Al alloy and Al<sub>2</sub>O<sub>3</sub>/6061Al composites in air [J]. *Material Science and Engineering*, 2006, A415, 80 - 86.
- [8] Timothy Mason J. Sonochemistry and sonoprocessing—the link, the trends and probably the future [J]. *Ultrasonics Sonochemistry*, 2003, 10, 175 - 179.
- [9] Zhang C L, Wu M S, Du J L, *et al.* Improving weld quality by arc-excited ultrasonic treatment [J]. *Tsinghua Science and Technology*, 2001, 6, 475 - 478.

**作者简介:** 张 平,男,1958 年出生,博士,教授,博士生导师. 主要从事焊接、离子注入等材料表面改性等方面的研究. 发表论文 50 余篇. Email: zhangp5801@sina.com

aohong<sup>3</sup>, WEI Yanhong<sup>1,3</sup> (1. State Key Laboratory of Advanced Welding Production Technology, Harbin Institute of Technology, Harbin 150001, China; 2. Shanghai Xin Li Institute of Power Equipment, Shanghai 200125, China; 3. School of Material Science and Technology, Nanjing University of Aeronautics & Astronautics, Nanjing 210016, China). p 17 – 20

**Abstract:** A software package has been developed which can simulate and predict the weld solidification cracks with three dimensional FEM. It consists of pre-processing, post-processing and solidification cracks predicting subsystem. The post-data treatment of software package for three-dimensional simulation and prediction of the weld solidification cracks can deal with the calculated results and display the results in featured curves, contours and 3D figures by combining graphic functions of softwares. The solidification cracks predicting subsystem regresses to the experimental data of transverse restraint test (TVT) to obtain the material resistance curve of weld solidification cracks or reads the modified material resistance of simulating TVT from the database and has it compared with the one and thus predict the weld metal solidification cracks.

**Key words:** solidification cracking; post-data treatment; material resistance curve; driving force

**Seam offset identification of underwater arc welding using PCA\_Nu-SVR** DU Jianhui, SHI Yonghua, WANG Guorong, HUANG Guoxing (South China University of Technology, School of Mechanical & Automotive Engineering, Guangzhou 510640, China). p 21 – 24

**Abstract:** In order to realize the underwater auto-welding based on rotating arc sensor and get high accuracy tracking, it is necessary to study the seam offset identification algorithm. First, the wavelet and median filter methods were used to process welding current signals, and then the signal was divided into cycle and normalized. PCA was used to remove the self-correlation of data set and reduce the number of inputs of Nu-SVR. The result showed that the maximum error and mean error of PCA\_Nu-SVR was 0.95 mm and 0.65 mm. The precision of PCA\_Nu-SVR was as good as Nu-SVR, and better than interval integral method and neural network. The runtime of PCA\_Nu-SVR was more than interval integral method, and less than neural network and Nu-SVR.

**Key words:** rotating arc sensor; underwater welding; principal component analysis; support vector regression; seam offset identification

**Parameters control for interfacial fracture mode of resistance spot weld dual-phase steels** YANG Haijun<sup>1</sup>, ZHANG Yansong<sup>1</sup>, LAI Xinmin<sup>1</sup>, ZHANG Xiaoyun<sup>2</sup> (1. School of Mechanical Engineering, Shanghai Jiaotong University, Shanghai 200240, China; 2. Vehicle Manufacturing Engineering, Shanghai General Motors, Shanghai 201201, China). p 25 – 28

**Abstract:** In this paper, the response surface method is used to analyze the influence of welding parameters on the interfacial fracture mode of resistance spot welded (RSW) joint made of dual phase steel DP600 with 1.4 mm thickness. The results showed that welding current, welding time and holding pressure were the key parameters to the interfacial fracture mode of the

RSW joints. The proper welding parameters can enlarge the weld nugget diameter ratio and reduce its sensitivity to welding parameters. The optimized welding parameters were obtained to control the interfacial fracture mode with the consideration of the robustness of welding process which was validated by experiments.

**Key words:** dual phase steel; interfacial fracture; improved response surface method; process optimization

**Synthetic analysis about effect of GMAW arc to Nd: YAG laser transmitting** WANG Wei, LIN Shangyang, WANG Xuyou, LEI Zhen (Harbin Welding Institute, Harbin 150080, China). p 29 – 32

**Abstract:** From the view of GMAW arc's absorption and refraction to Nd: YAG laser, the phenomena, which when Nd: YAG laser crosses GMAW arc, its radius will decrease, was analyzed in this paper. The results show that if decreasing of Nd: YAG laser radius is due to absorption of GMAW arc totally, the absorptivity of pulse GMAW arc to Nd: YAG laser is 0.7%, and the absorptivity of short-circuiting GMAW arc is 2.0%. If this phenomena is attributed to refraction of GMAW arc overall, Nd: YAG laser beam is deflected 0.34% by pulse GMAW arc, and 1.02% by short-circuiting GMAW arc. But considering this phenomena from the view of welding, it can regard approximately GMAW arc as no effect on Nd: YAG laser beam transmitting.

**Key words:** hybrid welding; laser welding; GMAW; laser absorption; laser refraction

**Digital welder parameters self-regulating algorithm based on partial Newton interpolation** LIN Fang<sup>1,2</sup>, HUANG Wenchao<sup>1</sup>, CHEN Xiaofeng<sup>1</sup>, WEI Zhonghua<sup>1</sup>, XUE Jiaxiang<sup>1</sup> (1. School of Mechanical & Automotive Engineering, South China University of Technology, Guangzhou 510640, China; 2. Department of Electromechanical Technology, Jiangmen Polytechnic, Jiangmen, Guangdong 529000, China). p 33 – 36

**Abstract:** A welding parameter self-regulating algorithm based on long-step calibration and partial Newton interpolation were put forward. By this algorithm, not only the unified parameters regulation could be realized, but also the database of the digital welder could be transformed from static mode into dynamic mode, in which the self-learning and self-regulating function were adopted. It might provide an effective strategy for the intelligent evolution of the digital welder. The results of the tests indicated that the welding parameters could be continuously self-regulated in a wide range. By the P-GMAW parameters generated by this algorithm, a stable welding process and well-formed seams could be acquired. By employing the parameter storing method with various priorities, the optimization of the parameters could be achieved.

**Key words:** digital welder; long-step calibration; partial Newton interpolation; self-regulating algorithm

**Experimental investigation of ultra-assisted electrode sparkles depositing process** ZHANG Pin<sup>1</sup>, MA Lin<sup>1,2</sup>, LIANG Zhijie<sup>2</sup> (1. Science and Technology Laboratory on Remanufacturing, Academy of Armored Force Engineering, Beijing 100072, China; 2. Institute of Chemical Defense, Beijing 102205, Chi-

na) . p 37 – 40

**Abstract:** Ultra-assisted electrode sparkle depositing ( UAESD) developed based on the traditional electrode sparkle depositing ( ESD) , and better coating could be achieved when ultrasonic vibration was adopted in the ESD technology. In this paper, UAESD was realized by the supersonic vibration of the body. The results showed that formation technological parameters were enlarged by supersonic vibration, and the better surface topography was achieved. The deposition efficiency increased 30% , microhardness increased 10% while the grain size decreased 24. 18% under the influence of the supersonic vibration. With the UAESD process, heat affected zone was enlarged and the microhardness at those points was increased. Moreover, the corrosion resistance of the bond was enhanced.

**Key words:** supersonic vibration; electrode sparkle depositing; strengthen coating

#### Research on fracture toughness of high-strength structural steel with prestrain at low temperature

XIAO Guangchun<sup>1,2</sup>, JING Hongyang<sup>1,2</sup>, XU Lianyong<sup>1,2</sup>, JI Jinchuan<sup>3</sup>, LI Wenliang<sup>3</sup> ( 1. School of Materials Science and Engineering, Tianjin University, Tianjin 300072, China; 2. Tianjin Key Laboratory of Advanced Joining Technology, Tianjin 300072, China; 3. Shanxi Electric Power Research Institute, Taiyuan 030001, China) . p 41 – 44

**Abstract:** The mechanical properties and fracture toughness of high-strength structural steel Q420 were studied by tension tests and three-point bending tests. The results indicated that the temperature had significant influence on fracture toughness of structural steel and the fracture toughness reduced significantly with the decrease of temperature resulting in brittle fracture. The prestrain increased the yield strength and tensile strength of structural steel, but significantly reduced its plasticity and fracture toughness, and further increased the possibility of brittle fracture. The prestrain facilitated the brittle fracture due to the activation of the near crack tip stress fields because of the prestrain based on the FEA. Thus the effects of the temperature and the prestrain should be considered in the important engineering design, material selection, safety analysis and evaluation.

**Key words:** high-strength structural steel; prestrain; mechanical properties; fracture toughness

#### Microstructure transformation and mechanical properties of electron beam welded joints of fusion CLAM steel

JIANG Zhizhong<sup>1</sup>, HUANG Jihua<sup>1</sup>, CHEN Shuhai<sup>1</sup>, JU Xin ( 1. School of Materials Science and Engineering, University of Science & Technology of Beijing, Beijing 100083, China; 2. School of Applied Science, University of Science & Technology of Beijing, Beijing 100083, China) . p 45 – 48

**Abstract:** China low activation martensitic ( CLAM) steel for fusion reactor were butt-welded through electron beam welding process, and followed by post-welding heat treatment ( PWHT) at 740 °C for 1 h. The microstructure and microhardness distribution of welded joints were analysed. The results showed that the weld seam with good formation and without appearance defects has been achieved. In as-welded condition, the weld metal and fusion zone consisted of a mixture of coarse lath martensite

and a little  $\delta$  ferrite. The coarse and fine grained zone was composed of fine lath martensite. The partially quenched zone mainly consisted of fine lath martensite and ferrite. The softening did not occur across welded joint. After PWHT, the lath martensite in the welded joint was transformed into tempered sorbite, which led to the significant decrease of the hardness of each zone. Among them, the highest hardness emerges at fusion zone was not at fine grained zone, which was just 20% higher than base metal. The PWHT did not make the tempered zone and base metal more soft obviously.

**Key words:** China low activation martensitic steel; electron beam welding; microstructure; microhardness

#### Influence of magnetic controlled technology on formation of high-speed TIG welding

CHANG Yunlong<sup>1</sup>, YANG Dianchen<sup>1</sup>, WEI Lai<sup>1</sup>, LU Lin<sup>2</sup> ( 1. Department of Material Science and Engineering, Shenyang University of Technology, Shenyang 110023, China; 2. Chemical Equipment College, Shenyang University of Technology, Liaoyang, Liaoning 111003, China) . p 49 – 52

**Abstract:** Increasing TIG welding speed may raise productivity. Welding speed increasing, however, will cause arc dragged backwards and anode spot delayed seriously. The two phenomena generate the defects of undercut and hump seam. As usual, the method of augmenting the shielding gas feed rate or increasing welding current was chosen to achieve it, but the ability to increase the welding speed was limited. The influence of transverse magnetic field on the welding speed, welding current and argon flow of high-speed TIG welding for austenite stainless steel were studied. The microstructure observation and flaring test were investigated. The experiment results indicated that welding speed could be increased from 3.5 m/min to 5.5 m/min, at the same time, welding current could be decreased from 95 A to 75 A, gas feed rate could be reduced from 0.7 m<sup>3</sup>/h to 0.5 m<sup>3</sup>/h, and the problems of undercut and hump seam due to high-speed TIG welding could be well solved.

**Key words:** high-speed TIG welding; magnetic field; undercut; flaring test

#### Microstructures and mechanical properties of Co-based surfacing alloys under DC transverse magnetic field

LIU Changjun<sup>1</sup>, LIU Zhengjun<sup>2</sup>, SU Ming<sup>2</sup>, SU Yunhai<sup>2</sup> ( 1. School of Chemical Equipment, Shenyang University of Technology, Liaoyang, Liaoning 111003, China; 2. School of Material Science and Engineering, Shenyang University of Technology, Shenyang 110870, China) . p 53 – 56, 60

**Abstract:** In order to improve the properties of surfacing layers, study the influence of surfacing current and magnetic field current on properties and microstructure of surfacing layer, DC transverse magnetic field was applied when Co-based alloy was welded on the surface of low-carbon steel by plasma arc surfacing. The hardness, wear resistance, microstructure and phase constitution of the surfacing layers were investigated via hardness and wear tests as well as SEM and XRD analysis. Furthermore, the influence of surfacing current and magnetic field current on the hardness and wear resistance of the surfacing layer were studied. The results showed that the properties of surfacing layers